Available online at www.sciencedirect.com

ScienceDirect

Procedia Engineering 175 (2017) 265 – 272

Procedia Engineering

www.elsevier.com/locate/procedia

1st International Conference on the Material Point Method, MPM 2017

A high order material point method

Roel Tielen[a,*], Elizaveta Wobbes[a], Matthias Möller[a], Lars Beuth[b]

[a] *Delft University of Technology, Mekelweg* 4, 2628 *CD Delft, the Netherlands*
[b] *Deltares, Boussinesqweg* 1, 2629 *HV Delft, the Netherlands*

Abstract

The classical material point method (MPM) developed in the 90s is known for drawbacks which affect the quality of results. The movement of material points from one element to another leads to non-physical oscillations known as 'grid crossing errors'. Furthermore, the use of material points as integration points renders a numerical quadrature rule of limited quality. Different solutions have been proposed in recent years to overcome these drawbacks. In this paper the approach of combining quadratic B-spline basis functions with a reconstruction based quadrature rule is pursued to solve these numerical problems. High-order B-spline basis functions solve the problem of grid crossing completely, whereas the considered reconstruction based quadrature rule reduces the quadrature error observed with MPM. In addition, the use of quadratic B-splines leads to a more accurate piecewise linear approximation of the stress field compared to the piecewise constant one obtained with linear Lagrangian basis functions commonly used with MPM. Two 1D benchmarks are considered involving large deformations, a vibrating bar and a column under self-weight. They render excellent results when adopting this high-order MPM.

Peer-review under responsibility of the organizing committee of the 1st International Conference on the Material Point Method
Keywords: material point method; B-splines; cubic splines.

1. Introduction

The MPM is a hybrid particle-mesh method [1,2]. It combines a fixed background mesh with a set of material points moving through the grid which discretize a deforming continuum. The material points store all information of the continuum such as density, stresses and strains. The mesh is used to solve the equations of motion of the continuum every time step after their assemblage from material point data.

Over the years, MPM has been used successfully for the simulation of a wide variety of complex engineering problems involving large deformations and history-dependent material behaviour such as sea ice dynamics [4] and slope failure [9].

The equations of motion may be solved in a variational framework adopting the finite element method (FEM) with linear C^0 Lagrange finite elements. The discontinuity of their gradients across element boundaries leads however to non-physical oscillations when material points cross element boundaries. This phenomenon, known as 'grid crossing error', significantly affects the quality of the MPM solution and may even lead to a lack of spatial convergence [5].

* Corresponding author.
E-mail address: roeltielen@hotmail.com

Peer-review under responsibility of the organizing committee of the 1st International Conference on the Material Point Method
doi:10.1016/j.proeng.2017.01.022

Different measures have been adopted as a remedy such as GIMP [6], the Dual Domain Material Point (DDMP) method [7] and mixed-integration approaches [8,9].
A further limitation to accuracy lies in the numerical integration. Material points are used as quadrature points and their volumes are interpreted as quadrature weights. The resulting numerical quadrature rule can be of very poor quality once material points become arbitrarily distributed. The use of standard quadrature rules such as Gaussian rules is not straightforward since physical quantities such as stresses and strains are only known at material point positions. Reconstruction techniques like the Moving Least Squares (MLS) approach [10] or interpolation as in [8,9] can be used to extend the discrete particle data to functions and apply standard quadrature rules on these to reduce the quadrature error of the MPM-type integration.
In this paper, a novel spline-based approach is proposed that combines high-order B-spline basis functions for the approximate solution of the equations of motion on the background grid with the improved accuracy of reconstruction-based numerical quadrature based on cubic spline interpolation.
Quadratic B-spline basis functions have continuous first derivatives which eliminate the effect of grid crossing errors entirely. Cubic spline interpolation of the discrete material point data and numerical integration by a sufficiently high Gauss quadrature rule reduces the integration error significantly. The performance of the novel MPM approach is demonstrated with 1D large deformation benchmarks.
In the following section, the devised spline-based MPM is described. Results obtained with spline-based MPM for different benchmarks are presented in Section 3. Conclusions are drawn in Section 4.

2. Spline-based MPM

In essence, the modifications of this approach are limited to the spatial discretization of the equations of motion on the background grid and the way in which integrals are evaluated numerically. The general MPM procedure has not been altered. It follows the formulation presented in [9] or [11] to which the reader is referred for a detailed description of MPM. Time integration is performed by the semi-explicit Euler-Cromer scheme [9].

2.1. Space discretization

B-spline basis functions of order d are uniquely defined by an underlying *knot vector* $\Xi = \{\xi_1, \xi_2, \ldots, \xi_{n+d+1}\}$ consisting of a set of non-decreasing *knots* ξ_i. A knot vector of length $n + d + 1$ defines n basis functions of order d. Constant B-spline basis functions are defined as:

$$\phi_{i,0}(\xi) = \begin{cases} 1 & \text{if } \xi_i \leq \xi < \xi_{i+1} \\ 0 & \text{else.} \end{cases}$$

Higher-order B-spline basis functions are then defined by the Cox-de Boor recursion formula [12]

$$\phi_{i,d}(\xi) = \frac{\xi - \xi_i}{\xi_{i+d} - \xi_i}\phi_{i,d-1}(\xi) + \frac{\xi_{i+d+1} - \xi}{\xi_{i+d+1} - \xi_{i+1}}\phi_{i+1,d-1}(\xi),$$

where $\xi \in [\xi_1, \xi_{n+d+1}]$. The non-empty intervals $[\xi_i, \xi_{i+1})$ are called *knot spans*. An open uniform knot vector is used, i.e. the knots are equally distributed and the first and last knots are repeated d times. Given an open uniform knot vector of length $n + d + 1$, the number of knot spans is equal to $n - d$. Quadratic B-spline basis functions are adopted. An example of quadratic B-spline basis functions derived from an open uniform knot vector is depicted in Figure 1.

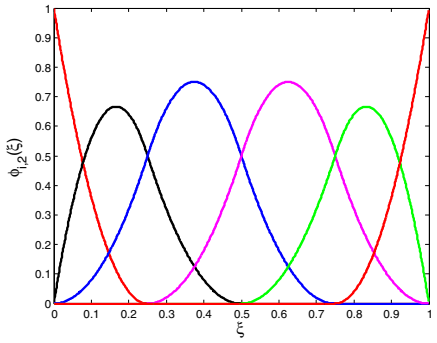

Fig. 1. Quadratic B-spline basis functions $\phi_{i,2}(\xi)$ based on the open uniform knot vector $\Xi = \{0, 0, 0, \frac{1}{4}, \frac{1}{2}, \frac{3}{4}, 1, 1, 1\}$.

B-spline basis functions of order d feature some amenable properties which make them ideal candidates for use with MPM:

- The basis functions $\phi_{i,d}$ are strictly positive over their entire support $[\xi_i, \xi_{i+d+1}]$ and possess the partition of unity property. The consistent mass matrix can therefore be safely replaced by its lumped counterpart as commonly done in MPM [1].
- The derivative of B-spline basis functions of order d is a linear combination of two B-spline basis functions of order $d - 1$. A quadratic approximation of the solution leads to a linear approximation of stresses instead of a constant approximation resulting from linear Lagrangian basis functions.
- The continuity of basis functions is C^{d-m_i}, where m_i denotes the multiplicity of the i-th knot. Hence, the use of quadratic B-spline basis functions based on an open uniform knot vector leads to basis functions with a continuous gradient. This solves the problem of grid crossing entirely.

Compared to standard Lagrange finite element-based MPM, the term 'element' has to be generalized to 'knot span'. The solution on the background grid found with quadratic B-spline basis functions at the position of the knots does not correspond to nodal values, e.g. $u_h(\xi_i) \neq u_i$, except at the boundary.

2.2. Numerical quadrature rule

Consider MPM-type integration of a function $f(x)$, which uses the material points x_p as quadrature points and the volume of the particle V_p as quadrature weights:

$$\int_\Omega f(x)\,\mathrm{d}\Omega \approx \sum_p V_p f(x_p) = \sum_p V_p f_p. \tag{1}$$

It should be noted that the function $f(x)$ is not available and only its values f_p at discrete particle positions are known. With reconstruction based quadrature, a function $\hat{f}(x)$ is constructed based on the discrete set of points $(x_p, f(x_p))$. The function $\hat{f}(x)$ is determined by cubic spline interpolation of the particle data. Integrals are then numerically approximated with a standard quadrature rule:

$$\int_\Omega f(x)\,\mathrm{d}\Omega \approx \sum_c \omega_c f(x_c) \approx \sum_c \omega_c \hat{f}(x_c). \tag{2}$$

Here, x_c denotes the position of the quadrature points and ω_c the corresponding quadrature weights. In this paper, integrals are approximated by applying a 2-point Gauss rule on the half of each non-zero interval $[\xi_i, \xi_{i+1}]$:

$$\int_\Omega f(x)\,\mathrm{d}\Omega = \sum_{j=d+1}^{n} \int_{\xi_j}^{\xi_{j+1}} f(x)\,\mathrm{d}\Omega \approx \sum_{j=d+1}^{n} \sum_{c=1}^{4} \omega_c f(x_c) \approx \sum_{j=d+1}^{n} \sum_{c=1}^{4} \omega_c \hat{f}(x_c). \tag{3}$$

In order to take the deformation of the continuum into account, the spline should only be reconstructed on the interval covered by the continuum. This interval Ω_t depends on the position and volume of the first and last particle and is approximately given by:

$$\Omega_t \approx [x_1 - \frac{1}{2}V_1, x_{n_p} + \frac{1}{2}V_{n_p}],$$

where n_p denotes the number of particles used to discretize the continuum. Quadrature points which do not lie in this interval obtain a function value of zero and, hence, do not contribute to the approximation of the integral. In case the boundary of the continuum does not coincide with a knot, the position of the Gauss points near the boundary are redefined. Figure 2 illustrates this procedure for an open uniform knot vector defined on $[0, L]$.

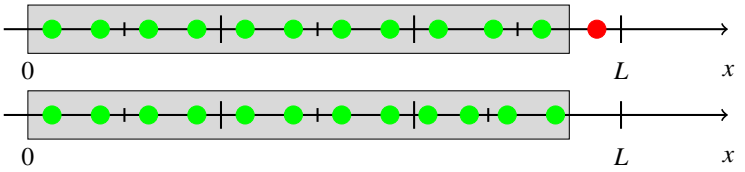

Fig. 2. Redefining position of the Gauss points based on the position of the continuum. The green and red dots denote respectively the active and inactive Gauss points, whereas the rectangle denotes the interval covered by the continuum.

Numerical integration is used with MPM to determine the mass matrix, force vectors and velocity at the degrees of freedom. With the devised spline-based MPM, the mass matrix and the gravitational force vector are still obtained by applying MPM-type integration. Thereby, mass is conserved when projecting the mass of the particles onto the degrees of freedom. Velocities in MPM are determined by a lumped density weighted L_2-projection of the momentum, which results in [11]:

$$\mathbf{v}_i^{t+\Delta t} = \frac{\mathbf{P}_{(i)}^{t+\Delta t}}{\mathbf{M}_{(i,i)}^{t}} \quad \text{with} \quad \mathbf{P}_{(i)}^{t+\Delta t} = \int_\Omega \rho(x) v(x)^{t+\Delta t} \phi_{i,d}(x)\, \mathrm{d}\Omega \quad \text{and} \quad \mathbf{M}_{(i,i)}^{t} = \int_\Omega \rho(x) \phi_{i,d}(x)\, \mathrm{d}\Omega. \tag{4}$$

The use of a consistent instead of a lumped mass matrix and a reconstruction based quadrature have been considered with the presented benchmarks. No definite choice could be made yet. Results obtained with the alternative projection are discussed for the two treated benchmarks. Reconstruction based quadrature is applied to determine the internal forces at degrees of freedom. The internal force at a single degree of freedom is computed by

$$\mathbf{F}_{(i)}^{\text{int}} = \int_\Omega \nabla\phi_{i,2}(x)\sigma(x)\, \mathrm{d}\Omega. \tag{5}$$

Based on the stresses at the material points a stress field $\hat{\sigma}(x)$ is constructed and the integral is numerically evaluated in the following way:

$$\mathbf{F}_{(i)}^{\text{int}} = \int_\Omega \nabla\phi_{i,d}(x)\sigma(x)\, \mathrm{d}\Omega \approx \sum_{j=d+1}^{n} \sum_{c=1}^{4} \omega_c \nabla\phi_{i,d}(x_c)\sigma(x_c) \approx \sum_{j=d+1}^{n} \sum_{c=1}^{4} \omega_c \nabla\phi_{i,d}(x_c)\hat{\sigma}(x_c). \tag{6}$$

3. Numerical results

The spline-based MPM has been implemented in Matlab. Results were obtained for two benchmarks involving dynamic large deformations of a linear-elastic material: a vibrating bar fixed at both ends and a column under self-weight. A variant of the first benchmark has been treated in [13]. Since no analytical solution is available for these large deformation benchmarks Updated Lagrangian FEM (ULFEM) calculations with sufficiently high numbers of degrees of freedom (DOF) are used as reference solutions with both benchmarks. An MPM making use of piecewise linear basis functions as presented in [9] or [11], referred to as standard MPM, was used for obtaining a reference computation with the first considered benchmark. With the second benchmark, results are compared to those obtained with the MPM code developed by the Anura 3D MPM Research Community [14] headed by Deltares, partner in this study.

3.1. Vibrating bar

This benchmark is concerned with the longitudinal vibrations of a bar fixed at both ends. Vibration is caused by initial velocities applied along the entire bar. The initial velocity is given by $v_0(x) = 0.1\sin\left(\frac{\pi x}{L}\right)$ [m/s]. No gravitational force is applied. The length L of the bar is 1 [m], the Young's modulus E is 50 [Pa] and the density ρ is 25 [kg/m^3]. A maximum deformation is observed at the middle of the bar of approximately 0.02 m. The bar is discretized by 32 knot spans, the initial number of material points per knot span is 4. Material points are initially equidistantly distributed over the domain. A time step size of $\Delta t = 1 \cdot 10^{-5}$ [s] is used which corresponds to a low CFL number of $3.2 \cdot 10^{-3}$. A low Courant number is used to minimize the influence of the semi-explicit Euler-Cromer time-integration scheme [9] on the accuracy of the results. Velocities at the DOF are determined by making use of a consistent mass matrix and a reconstruction based quadrature. The explicit solution of the linear system is avoided by adopting Richardson iteration [15].

Figure 3 shows the internal force at a single degree of freedom over time obtained with standard MPM and spline-based MPM. The red line at the bottom indicates the occurrence of grid crossings which coincides with an instantaneous increase (or decrease) of the internal force when adopting linear Lagrange basis functions entailing, as can be seen, a further non-physical development of the internal force over time. These instantaneous increases (or decreases) are not found with spline-based MPM. Numerical experiments described in [11] show that the use of quadratic B-spline basis functions is sufficient to solve the problem of grid crossing. In Figure 4 stresses across the bar at time $t = 0.5$ s are shown. Those on the left are obtained with standard MPM, stresses shown on the right with spline-based MPM. Grid crossings result in severe unrealistic stress oscillations at the material points. Spline-based MPM leads to a piecewise linear stress field which corresponds well to the reference solution obtained with ULFEM.

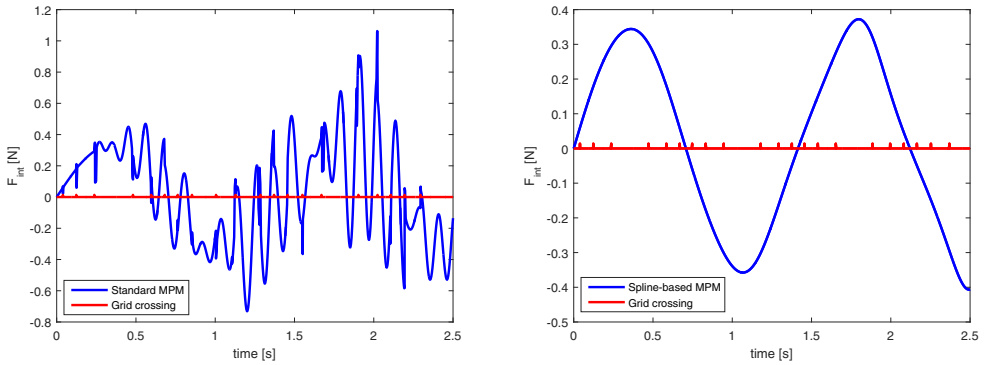

Fig. 3. Internal force at a degree of freedom over time with standard MPM (left) and spline-based MPM (right).

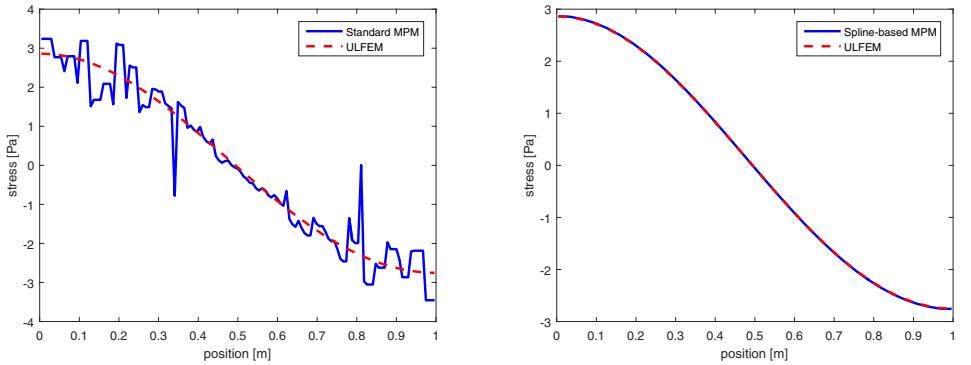

Fig. 4. Stresses across the bar at time $t = 0.5$ s with standard MPM (left) and spline-based MPM (right).

3.2. Column under self-weight

A gravitational force is instantaneously applied along a column. Results are compared with those obtained with a 3D MPM code, Anura 3D [14], making use of linear Lagrange basis functions and a mixed-integration technique to mitigate grid crossing and integration errors [8,9]. A 1D benchmark is obtained with this 3D code when setting the Poisson's ratio equal to 0.

The initial height of the column H is 1 [m] and the Young's modulus E is $1 \cdot 10^5$ [Pa]. The density ρ is $1 \cdot 10^3$ [kg/m^3] and the gravitational acceleration g is 9.81 [m/s^2]. The column is discretized by 32 knot spans with spline-based MPM and by 352 4-noded tetrahedral elements with Anura 3D arranged in 32 layers. A low CFL number of 0.065 is used for all computations.

In contrast to the previous benchmark, entries of the consistent mass matrix approach zero during the simulation since the column is free at one end. Utilization of a consistent mass matrix then leads to unrealistically high velocities at the DOF when solving the momentum equation. Therefore, velocities at the DOF are obtained by making use of a lumped mass matrix, thereby exploiting the partition of unity property of B-spline basis functions, and an MPM-type quadrature.

The velocity of the material point situated at the column center is shown in Figure 5. Results on the left are obtained with Anura 3D and ULFEM. Results on the right are obtained with spline-based MPM and ULFEM. In contrast to standard MPM considered in Section 3.1, Anura 3D makes use of mixed-integration approaches [8,9] so that no oscillations occur. The solution obtained with spline-based MPM is almost identical to the solution obtained with Anura 3D.

Figure 6 shows the stress of the same material point over time. The stress obtained with spline-based MPM and Anura 3D correspond well with the ULFEM solution.

Figure 7 depicts the stresses along the column at time $t = 0.5$ [s]. For both, Anura 3D and spline-based MPM, again good agreement is found with the ULFEM solution. However, spline-based MPM renders a piecewise linear stress field instead of a constant one.

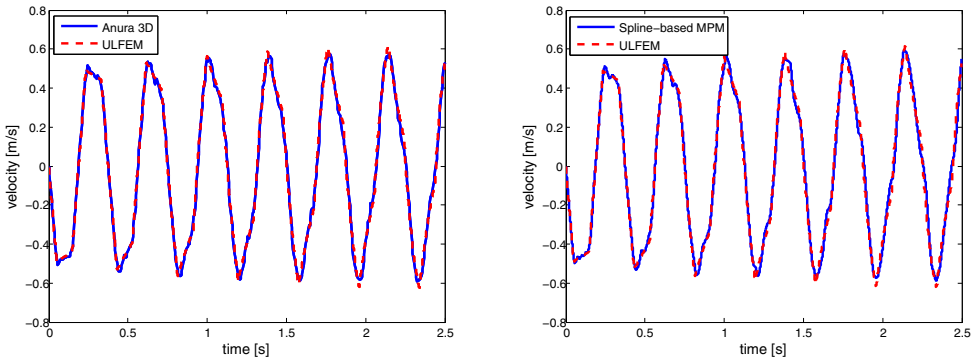

Fig. 5. Velocity of material point at column center over time obtained with Anura 3D (left) and spline-based MPM (right).

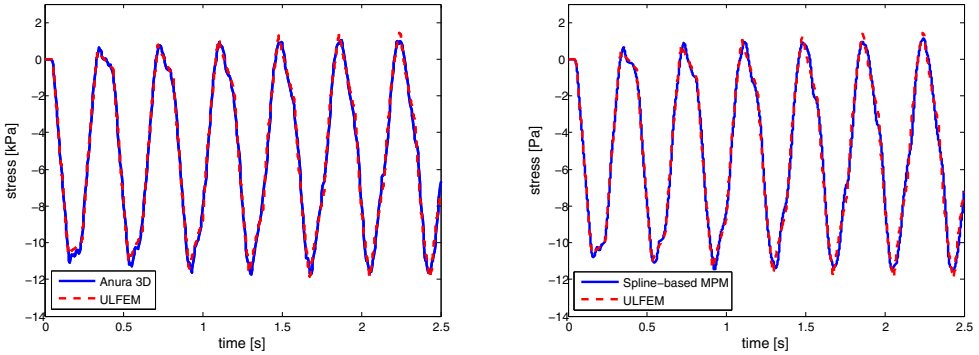

Fig. 6. Stress of material point at column center over time obtained with Anura 3D (left) and spline-based MPM (right).

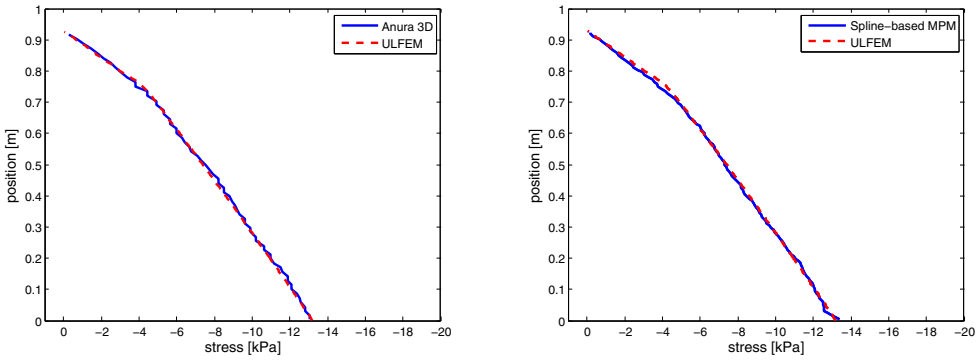

Fig. 7. Stresses along the column at time $t = 0.5$ s obtained with Anura 3D (left) and spline-based MPM (right).

4. Conclusions

In this paper, a novel spline-based MPM approach has been presented that combines the use of quadratic B-spline basis functions with a reconstruction based quadrature rule. The considered 1D benchmarks render excellent results. High-order B-spline basis functions with continuous gradients solve the problem of grid crossing completely. In addition, a more accurate piecewise linear approximation of stresses can be obtained with quadratic B-spline basis functions. The reconstruction based quadrature ensures a 'constant' quality of the numerical quadrature when material points become arbitrarily distributed.

It was found that the way in which velocities at the DOF are computed has a significant influence on numerical results. Two approaches have been pursued. The use of a consistent mass matrix and a reconstruction based quadrature rule are necessary to obtain a solution for the first benchmark without oscillations at the boundary. The alternative velocity projection leads to a spatial convergence of $O(h^3)$ with this benchmark [11]. A drawback of this alternative projection arises when entries of the mass matrix approach zero, leading to unrealistic high velocities at corresponding DOF. The use of a lumped mass matrix and MPM-type integration provide an accurate solution for the second benchmark even if entries of the mass matrix approach zero.

Further research remains to be done to devise a solution on a velocity projection which combines the advantages of both projections, while minimizing their drawbacks. For using spline-based MPM for practical problems, extension to 2D and 3D is necessary. Further research will focus on these aspects as well and, beyond that, on the application of spline-based MPM to advanced geotechnical problems.

References

[1] D. Sulsky, S. Zhou, H. Schreyer, Application of a particle-in-cell method to solid mechanics, Computer Physics Communications. 87 (1995) pp. 236–252
[2] D. Sulsky, Z. Chen, H. Schreyer, A particle method for history-dependent materials, Computer methods in applied mechanics and engineering. 118 (1994) pp. 179–196
[3] D. Zhang, Q. Zou, B. VanderHeyden, X. Ma. Material point method applied to multiphase flows. Journal of Computational Physics. 227 (2008) pp. 3159—3173
[4] D. Sulsky, H. Schreyer, K.Peterson, R. Kwok, M. Coon. Using the material point method to model sea ice dynamics. Journal of Geophysical Research. 112 (2007)
[5] M. Steffen, R. Kirby, M. Berzins. Analysis and reduction of quadrature errors in the material point method (mpm). International journal for numerical methods in engineering. 76 (2008) pp.922–948
[6] S. Bardenhagen, M. Kober. The generalized material point method. Computer Modelling in Engineering and Sciences. 5 (2004) pp. 477–495
[7] D.Z. Zhang, X. Ma, P.T. Giguere. Material point method enhanced by modified gradient of shape function. Journal of Computational Physics. 230 (2011) pp. 6379–6398
[8] L. Beuth. Formulation and Application of a Quasi-Static Material Point Method. Phd thesis. University of Stuttgart (2012)
[9] I. Al-Kafaji. Formulation of a Dynamic Material Point Method (MPM) for Geomechanical Problems. Phd thesis. University of Stuttgart (2013)
[10] M. Gong. Improving the Material Point Method. Phd thesis. The University of New Mexico. (2015)
[11] R. Tielen. A High-Order MPM. Master's thesis. Delft University of Technology. (2016)
[12] T.R. Hughes, J.A. Cottrell, Y. Bazilevs. Isogeometric analysis: , finite elements, NURBS, exact geometry and mesh refinement. Computer Methods Applied Mechanical Engineering 194 (2005) pp. 4135–4195
[13] S. Bardenhagen. Energy conservation error in the material point method for solid mechanics. Journal of Computational Physics 180 (2002) pp.383–403
[14] http://www.anura3d.com/
[15] D. Kuzmin, M. Möller, N. John, M. Shashkov. Failsafe flux limiting and constrained data projection for equations of gas dynamics. Journal of Computational Physics 229 (2010) pp. 8766–8779